CONF-790816--57

STUDIES RELATED TO EMERGENCY DECAY HEAT REMOVAL IN EBR-II

by

Ralph M. Singer, Jerry L. Gillette, Dale Mohr,
John V. Tokar, John E. Sullivan and Eric M. Dean

MASTER

Prepared for

ANS/ENS International Meeting

on

Fast Reactor Safety Technology

Seattle, Washington

August 19-23, 1979

U of C-AUA-USDOE

ARGONNE NATIONAL LABORATORY, ARGONNE, ILLINOIS

Operated under Contract W-31-109-Eng-38 for the

U. S. DEPARTMENT OF ENERGY

STUDIES RELATED TO EMERGENCY DECAY HEAT REMOVAL IN EBR-II

Ralph M. Singer, Jerry L. Gillette, Dale Mohr,
John V. Tokar, John E. Sullivan, and Eric M. Dean

EBR-II Project
Argonne National Laboratory
Argonne, Illinois and Idaho Falls, Idaho

ABSTRACT

Experimental and analytical studies related to emergency decay heat removal by natural circulation in the EBR-II heat transport circuits are described in this paper. Three general categories of natural circulation plant transients are discussed and the resultant reactor flow and temperature response to these events are presented. These categories include the following: (1) loss of forced flow from decay power and low initial flow rates; (2) reactor scram with a delayed loss of forced flow; and (3) loss of forced flow with a plant protective system activated scram. In all cases, the transition from forced to natural convective flow was smooth and the peak in-core temperature rises were small to moderate. Comparisons between experimental measurements in EBR-II and analytical predictions of the NATDEMO code are included.

INTRODUCTION

During the normal operation of a liquid-metal-cooled fast-breeder reactor (LMFBR), fuel and component temperatures are controlled within prescribed limits by the forced circulation of liquid sodium. However, during certain events postulated to occur during the operating lifetime of a reactor plant, electrical power to the coolant pumps can be lost. This will result in a run-down of the primary pumps and a corresponding loss of forced flow. As the forced flow in the primary system starts to decrease, the plant protective system will, with extremely high reliability, shut down the plant. However, due to the generation of radioactive material within the fuel and structural components of the reactor during power operation, a certain amount of residual decay heat will be released, even though the primary fission reactions have ceased. Therefore, there must be some continued circulation of coolant following this event, albeit at a much reduced rate, in order to prevent undesirable temperatures being reached.

Prudent engineering design necessitates the inclusion of at least one back-up system to provide sufficient coolant flow through the main heat transport circuits in order to maintain reactor temperatures within prescribed limits. Particular systems which have been designed include pony-motors on the primary pumps powered by diesel generators, auxiliary pumps driven by storage batteries, or other related concepts, all of which provide some form of emergency electrical or mechanical energy supplies. However, in order to assure continued reactor coolability even in the extremely remote event of a complete operational failure of these types of engineered safeguards, the main heat transport circuits of the plant, as well as any separate decay heat removal circuits, should be designed to promote natural circulation of the coolant. Thus, the inherent natural circulation capability of a plant is an ultimate, "fall-back" heat transport mechanism of emergency decay heat removal.

In the Experimental Breeder Reactor II (EBR-II), emergency forced pumping of the primary coolant is provided by an auxiliary electromagnetic pump which is located in hydraulic series with the primary pumps and normally operated by site power, but is also backed up by a diesel generator, and directly tied into a bank of storage batteries. Thus, even in the remote event of a complete loss of on-site electrical power (including the inability to start the diesel generator), continued forced flow through the reactor can be maintained by the auxiliary pump at levels sufficient to remove decay heat using the energy stored in the batteries so that a smooth transition to natural convective flow ultimately occurs. The decay heat is then normally convected through the normal heat transport circuits and dissipated to the atmosphere by the condenser water cooling tower. As a back-up to this mode of decay heat removal which is independent of the secondary sodium system, two natural-convective-driven NaK immersion coolers are located within the primary pool and transfers heat to air via a natural-air-draft cooler. Additional details on these EBR-II systems can be obtained from Ref. [1].

The purpose of this paper is to summarize the results of the work conducted at EBR-II which addresses the natural circulation performance of the normal heat transport circuits in the plant. These efforts include analytical modeling as well as direct total plant testing. A series of steady-state natural circulation tests were conducted and reported earlier [2] and a review of related studies was described in [3]; therefore, emphasis here will be on the transient tests conducted at EBR-II. These tests were primarily directed toward developing an understanding of the dynamics of the transition from forced to natural convective flow and included the following categories of experiments:

1) loss of primary forced flow from decay power and low initial flow rates,
2) reactor scram with a delayed loss of primary forced flow, and
3) loss of primary forced flow from fission power with resultant PPS activated reactor scram.

Typical measured and calculated transient coolant flow rates and temperatures for each of these three types of events will be presented and discussed. The predicted reactor behavior was obtained through use of the primary system module of the NATDEMO code [4].

REACTOR AND INSTRUMENTATION DESCRIPTION

The Experimental Breeder Reactor II (EBR-II) is a sodium-cooled fast breeder reactor with a complete steam-electric system. The plant is located in the Idaho National Engineering Laboratory (INEL) and is operated by Argonne National Laboratory for the U. S. Department of Energy. The reactor consists of 16 rows of subassemblies, the inner 7 constituting the fueled core and the outer nine containing reflector and blanket subassemblies. The active fuel length in the core is 0.343 m, with 91 elements in a metal fuel driver subassembly. These driver fuel elements are 4.42 mm in diameter and are contained within a hexagonal can which has a flat-to-flat internal dimension of 56.1 mm. The spacing of the individual fuel elements is maintained by wire wraps with a diameter of 1.24 mm and an axial pitch of 152 mm. The normal operating power of the reactor is 60.0 MWt at a total primary coolant flow rate of 0.516 m^3/s. The plant consists of a single intermediate heat exchanger (IHX) and an associated secondary system. Superheated steam is provided to a single turbine-generator utilizing multiple evaporator and superheater units. The evaporators operate with natural recirculation. Additional descriptive information on EBR-II is available in [1] and a sketch of the primary heat transport circuit is shown in Fig. 1.

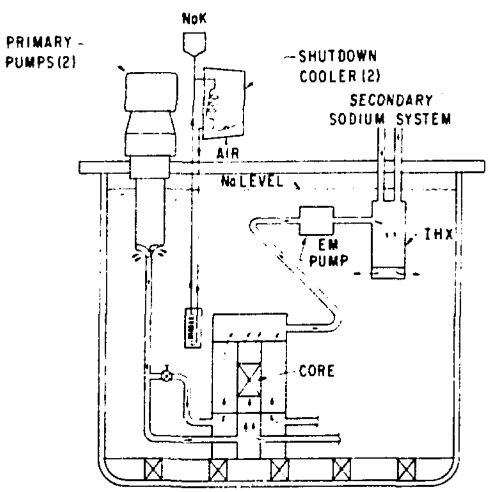

Fig. 1. Sketch of the EBR-II Primary System

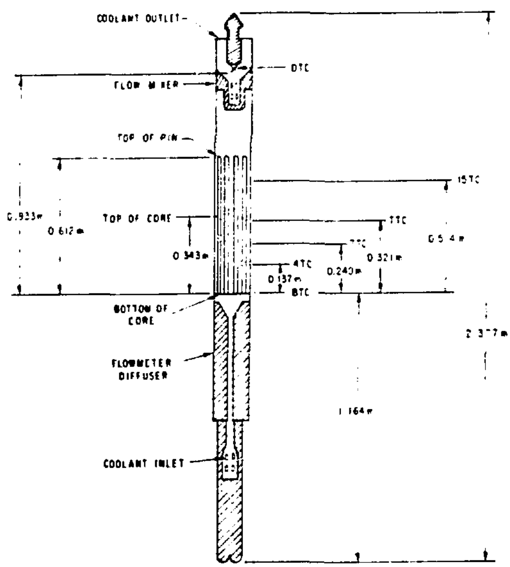

Fig. 2. Sketch of the Instrumented Fuel Subassembly, XX08

The instrumentation utilized in the EBR-II tests includes both the normal plant sensors and special in-core sensors. The in-core instrumentation was located in a modified driver subassembly placed in a converted control-rod position in the fifth row of the core. This experimental subassembly, designated XX08, consists of 61 elements, 58 of which are fueled, and are contained within a hexagonal can which measures 46.4 mm across its inside flats resulting in a pin bundle hydraulic diameter of 2.76 mm. Within this subassembly, there are two inlet, permanent magnet flowmeters, six fuel centerline thermocouples, referred to as "FTC," located 21.6 mm below the top of the fuel at beginning of fuel life (or 0.321 m above core bottom), and 16 coolant thermocouples mounted as wire wrap spacers. Two of these coolant thermocouples, called "BTC," are located at the core bottom, two, called "4TC," are at 0.4 of the core height (0.137 m above core bottom), two, called "7TC," are at 0.7 of the core height (0.240 m above core bottom), nine, called "TTC," are near the core top (same height as the fuel thermocouples), and one, called "15TC," is at 1.5 of the core height (0.514 m above core bottom or 0.171 m above core top). In addition, two coolant thermocouples, called "OTC," are located above a flow mixer near the subassembly exit, but within the hex can and 0.933 m above core bottom, and measure the mixed-mean coolant outlet temperature. A schematic diagram indicating the axial location of the XX08 instrumentation is shown in Fig. 2. Additional details on the instrumented subassembly XX08 are available in [5].

The general plant instrumentation is calibrated on a periodic basis; however, special calibration efforts were undertaken for the tests reported in this paper. The temperature sensors (including both thermocouples and resistance thermometers) and their associated signal conditioning equipment were checked for off-sets for each test by operating the plant at full (100%) flow and extremely low decay power. This resulted in an isothermal primary system (except for the slight temperature rise across the core which was accounted for) and all of the signals from the temperature sensors could thereby be corrected. With only a few exceptions, the corrections obtained from this calibration were less than 1 C, and therefore, it is felt that all of the temperature measurements herein reported have uncertainties of less than about ±0.5 C. Although the flowmeters were not calibrated in-place, extensive out-of-pile sodium calibration tests were performed for those units located within the XX08 subassembly. Thus the sensitivity of these flowmeters is known explicity over the range of about 0.3×10^{-4} to 25×10^{-4} m^3/s (about 1 to 100% of full flow), and was obtained for lower flow rates by extrapolation between 0 and 0.3×10^{-4} m^3/s. The calibration uncertainty was estimated to be about ±0.2% for flow rates greater than about 6×10^{-4} m^3/s, about ±1% for flow rates between 0.3×10^{-4} and 0.6×10^{-4} m^3/s, and about ±5% for lower flow rates. Because of the additional uncertainties involved with the signal conditioning equipment and the actual reactor environment, it is estimated that the final reported flow rates have inherent uncertainties of about twice these calibration values.

LOSS OF FORCED FLOW JUST PRIOR TO FUEL HANDLING

Experiments of this category were designed to investigate the response of a plant to a loss of on-site electrical power shortly following a reactor shutdown in preparation for fuel handling. In this situation, it is postulated that the reactor is being cooled by forced circulation of the primary coolant through operation of either pony motors or auxiliary pumps, and the decay heat load corresponds to levels appropriate for shutdown periods of tens of minutes to several days. From these initial conditions of low flow rate and low power, the transient is initiated by a loss of pumping power and a subsequent transition to natural circulation. For the purposes of this paper, the details of one particular test will be described as representative of this class of transients.

The initial conditions of this test were a decay power level of 1.6% and a forced flow rate of 5.3% of rated supplied by a primary auxiliary pump. The electrical power to the auxiliary pump was abruptly disconnected, and since this pump is a simple open-tube electromagnetic design, the resulting flow coastdown was rapid and depended only upon the primary system fluid inertia. The resulting thermal-hydraulic response of the reactor is illustrated by the in-core measurements shown in Fig. 3. The coolant flow rate in an instrumented fueled subassembly is seen to drop from its initial value of 5.3% to about 0.7% within 20 s, and then gradually increase to 1.2 to 1.3% as buoyancy forces develop. The corresponding coolant temperature at the top-of-core location rises to a peak of 513 C (the inlet temperature was 371 C) at 60 s, and then slowly declines thereafter. The corresponding predictions by the NATDEMO code are superimposed on these measurements; it should be mentioned that the predictions are based upon the behavior of the average core while the measurements are, of course, made in a particular subassembly whose thermal-hydraulic parameters differ somewhat from the average.

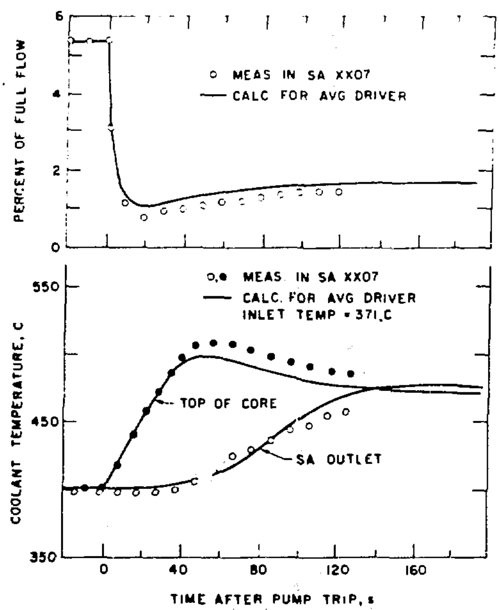

Fig. 3. Thermal and Hydraulic Core Response to a Transition to Natural Convection from Low Power and Flow Conditions

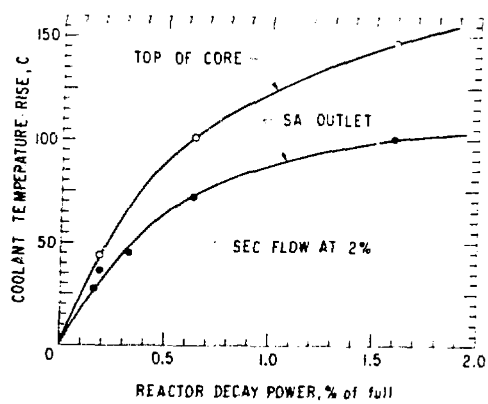

Fig. 4. Dependance of the Peak Transient Coolant Temperatures at Core Top and Subassembly Outlet Upon the Reactor Decay Power.

As mentioned earlier, a series of tests of this type were conducted in which the effect of reactor decay power upon peak in-core temperatures were measured. A summary of these results for the subassembly outlet and top-of-core locations is shown in Fig. 4. In contrast to forced convection transients, in which a similar plot of the peak temperature rise versus reactor power would be linear, these natural circulation transients exhibit a strong non-linear peak transient temperature versus power relationship. This is simply due to the fact that although the increased power tends to result in higher coolant temperatures, the higher coolant temperatures result in larger buoyancy forces and therefore somewhat higher coolant velocities. Thus, in natural circulation transients, the system inherently tends to mitigate the effects of power changes.

REACTOR SCRAM WITH DELAYED LOSS OF FORCED FLOW

If a plant experiences a reactor scram followed very shortly thereafter by a complete loss of forced flow, a potentially adverse condition for the establishment of natural convection may exist. For example, if the delay in the loss of forced flow after reactor scram is sufficiently long, or the plant has a very long primary pump rundown time, the primary heat transport circuit can be cooled down to near the nominal inlet temperature, and only the buoyant forces generated by heating of the coolant in the core can accelerate the relatively cold, dense fluid in the heat transport circuits. Under these conditions, it is expected that the transient flow rate would be less than that resulting when the coolant temperatures in the heat transport circuits are higher. The peak temperatures reached may be either higher or lower, depending upon the actual decay heat level and the detailed plant design.

In order to examine the dynamics of the transition from forced to natural convection flow under these conditions, several plant tests were conducted, typically in the following manner: power operation was terminated by a reactor scram with the primary pumps left on; after the primary heat transport system had cooled down and the decay heat reached a predetermined value, all forced flow was stopped by interrupting power to the primary pumps. The resulting flow coastdown and temperature transient resulting from a typical test in which the initial flow rate was 34%, the decay power 0.73%, and the inlet temperature 363 C, is shown in Fig. 5. As was expected, the flow rate drops to a very low value (about 0.23%), and then recovers to above 1.0% as the coolant in the core and heat transport circuits heat up. The top of core and subassembly outlet coolant temperature transients indicate significantly slower rise times than were experienced in the low power and low flow transients, but higher peak values are reached due to the adverse convective flow conditions. For example, while the peak top-of-core coolant temperature rise reached in this test (from Fig. 5) was 92 C, a test conducted with identical decay power and balance-of-plant conditions, but with a larger initial temperature rise (due to a smaller initial flow rate) resulted in a peak rise of only 53 C. These observations suggest that continued forced primary flow, or equivalently, extended primary pump rundown times, following a reactor scram may be an undesirable design feature relative to the natural convective performance of a plant.

The calculated flow and coolant temperature transient for an average driver subassembly using the NATDEMO code is also shown in Fig. 5. The experimental and analytical comparison is seen to be quite good, especially since the thermal and hydraulic parameters of the instrumented subassembly are somewhat different from an average driver.

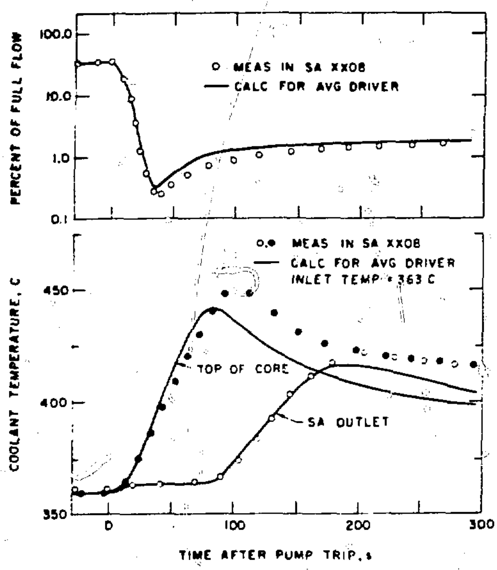

Fig. 5. Thermal and Hydraulic Core Response to a Transition to Natural Convection with Reactor Scram Preceding Loss of Forced Flow

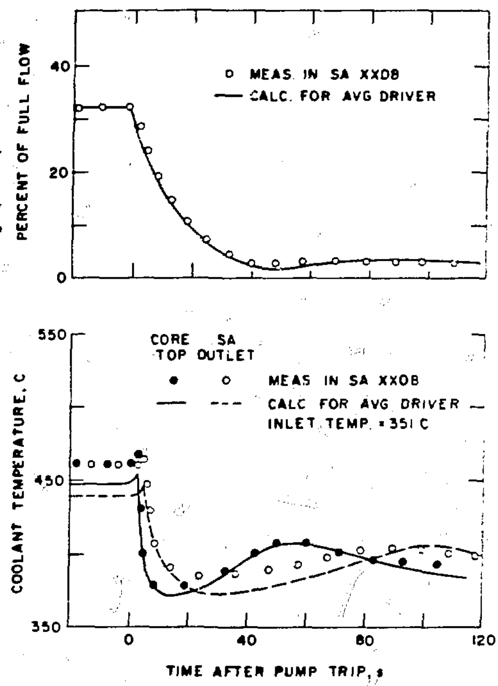

Fig. 6. Thermal and Hydraulic Core Response to a Transition to Natural Convection with Reactor Scram Caused by a Loss of Forced Flow

LOSS OF FORCED FLOW CONCOMITANT WITH REACTOR SCRAM

A more commonly analyzed natural circulation event than those previous described is that corresponding to a complete loss of on-site power during normal plant operation. During this event, a complete loss of all forced flow is assumed to occur; the reactor is then automatically scrammed by the plant protection system responding to a low flow signal. During the resulting combined power and flow transient, the normalized power-to-flow ratio initially drops below unity, then can increase above unity, and finally monotonically decreases as convective flow develops. The actual range of the power-to-flow ratio, as well as the lagging core temperatures, during this type of transient depend strongly upon many plant parameters, particularly the primary pump run-down time and its relationship to the secondary system dynamics and the heat transport circuit geometry and hydraulic characteristics.

Since the physical design of EBR-II cannot be conveniently altered, the latter effect could not be studied. However, the former and many other parametric effects were experimentally examined. The details of one of the tests of this category will be described as illustrative of the core response to a complete loss of primary forced flow from an at-power condition. The initial operating power and flow values of 28.5% and 32.1% (corresponding to a core temperature rise of 90 C above the inlet level of 351 C) were maintained for about 3 hours in order to permit the build-up of sufficient short-lived radio-isotopes to provide a reasonably prototypic decay heat transient following reactor scram. Immediately prior to the scram, the power to the primary auxiliary pump was disconnected; continued forced primary flow could then be provided only by the primary pumps. The transient was initiated by interrupting the power to the primary pumps; this resulted in an immediate flow coastdown and a subsequent automatic reactor scram. The secondary system pump was permitted to remain in operation during this test.

A typical measured in-core coolant flow rate and temperature transient resulting from this event are shown in Fig. 6. Also indicated are the predictions from the system code, NATDEMO, for an average driver subassembly. Following the loss of pumping power, the coolant flow rate drops from its initial value of 32.1% to a minimum of 2.8% in 43 s, then recovers slightly and finally slowly decreases as the fission-product inventory in the reactor decays. The coolant temperature at core top in the instrumented subassembly is seen to initially rise during the period between the loss of flow and reactor scram. The rapid decrease follows the scram, and the subsequent rise and decline follows the relative values of the decaying power and developing natural convective flow. Similar behavior is seen at the subassembly outlet location, with the exception of the changes being considerably damped primarily due to the above-core structural heat capacity. The maximum top-of-core coolant temperature rise measured during this transient is seen to be 62 C as compared to the initial temperature rise of 113 C. The maximum transient value predicted by NATDEMO in an average driver subassembly for this test was 63 C.

CONCLUSIONS

A number of transient natural circulation tests were conducted in EBR-II utilizing the availability of active in-core and plant sensors. These tests examined the response of the plant to postulated loss-of-flow operational events which could occur just prior to fuel handling, just after a reactor scram, or during at-power operation. In all cases, very smooth transitions from forced to natural convective flow occurred, and the reactor decay heat was transferred through the normal heat transport circuits without causing the in-core temperatures to reach undesirable levels. Analyses performed using the EBR-II system simulation code, NATDEMO [4], resulted in predicted coolant flow rates and temperatures which agreed quite well with the measurements.

ACKNOWLEDGMENTS

These whole plant natural circulation transients could not have been successfully conducted without the direct technical support of many EBR-II personnel. We would like to especially acknowledge Roland Smith, William Perry, Gary Lentz, and all of the reactor operating crews for their efforts related to the many operational problems involved with these tests, William Booty for his work in developing the data acquisition programs, Nadine Allen and Lavar Welker for their work in procedures and scheduling, and the many EBR-II experimenters who agreed to having their experimental irradiation subassemblies ride through these thermal-hydraulic transients. This work was supported by the U. S. Department of Energy.

REFERENCES

1. Koch, L. J., et al., "Hazard Summary Report: Experimental Breeder Reactor II (EBR-II), Argonne National Laboratory Report No. ANL-5719 (May 1957) and ANL-5719 (Addendum) (June 1962).

2. Singer, R. M., et al., "Steady-State Natural Circulation Performance of the EBR-II Primary Heat Transport Circuit," Nuc. Sci., and Eng. 63, pp. 75-82 (1977).

3. Singer, R. M., D. Grand, and Martin, R., "Natural Circulation Heat Transfer in Pool-Type LMFBR's," Proc. Symp. Thermal and Hydraulic Aspects of Nuclear Reactor Safety, Vol. 2: LMFBR, eds. O. C. Jones and S. G. Bankoff, ASME (Nov. 1977) pp. 239-264.

4. Mohr, D. and Feldman, E. E., "A Dynamic Simulation of the EBR-II Plant with the NATDEMO Code," presented at this conference.

5. Smaardyk, A., et al., "EBR-II Environmental Instrumented Subassembly XX08: Engineering and Assembly," Argonne National Laboratory Report ANL-78-9 (May 1978).